ELSEVIER

**doi:10.1016/j.ijrobp.2004.05.048**

---

**CLINICAL INVESTIGATION**                                                                            **Liver**

---

# BIOLOGIC SUSCEPTIBILITY OF HEPATOCELLULAR CARCINOMA PATIENTS TREATED WITH RADIOTHERAPY TO RADIATION-INDUCED LIVER DISEASE

JASON CHIA-HSIEN CHENG, M.D., M.S.,*,†,‡ JIAN-KUEN WU, M.S.,‡,§ PATRICIA CHIAO-TZU LEE, M.S.,‡
HUA-SHAN LIU, M.S.,* JAMES JER-MIN JIAN, M.D.,† YU-MONG LIN, M.D.,‖ JUEI-LOW SUNG, M.D.,‖
AND GWO-JEN JAN, PH.D.*

*Department of Electrical Engineering, National Taiwan University, Taipei, Taiwan; Departments of †Radiation Oncology,
§Medical Physics, and ‖Internal Medicine, Koo Foundation Sun Yat-Sen Cancer Center, Taipei, Taiwan; ‡Cancer Research Center
and Division of Radiation Oncology, Department of Oncology, National Taiwan University Hospital and National Taiwan
University College of Medicine, Taipei, Taiwan

**Purpose: To identify the factors associated with radiation-induced liver disease (RILD) and to describe the difference in normal tissue complication probability (NTCP) between subgroups of hepatocellular carcinoma patients undergoing three-dimensional conformal radiotherapy (3D-CRT).**

**Methods and Materials: A total of 89 hepatocellular carcinoma patients who completed 3D-CRT for local hepatic tumors were included. The average isocenter dose was $49.9 \pm 6.2$ Gy. Logistic regression analysis was used for the association between statistically significant factors and RILD (defined as Grade 3 or 4 hepatic toxicity of elevated transaminases or alkaline phosphatase within 4 months of completing 3D-CRT) in multivariate analysis. Maximal likelihood analysis was conducted to obtain the best estimates of the NTCP model parameters.**

**Results: Of the 89 patients, 17 developed RILD. In univariate analysis, hepatitis B virus (HBV)-positive status and the mean radiation dose to the liver were the two factors significantly associated with the development of RILD. Of the 65 patients who were HBV carriers, 16 had RILD compared with 1 of 24 non–carrier patients ($p = 0.03$). The mean radiation dose to liver was significantly greater in patients with RILD (22.9 vs. 19.0 Gy, $p = 0.05$). On multivariate analysis, HBV carrier status (odds ratio, 9.26; $p = 0.04$) and Child-Pugh B cirrhosis of the liver (odds ratio, 3.65; $p = 0.04$) remained statistically significant. The best estimates of the NTCP parameters were n = 0.35, m = 0.39, and $TD_{50}(1) = 49.4$ Gy. The n, m, $TD_{50}(1)$ specifically estimated from the HBV carriers was 0.26, 0.40, and 50.0 Gy, respectively, compared with 0.86, 0.31, and 46.1 Gy, respectively, for non–carrier patients.**

**Conclusion: Hepatocellular carcinoma patients who were HBV carriers or had Child-Pugh B cirrhosis presented with a statistically significantly greater susceptibility to RILD after 3D-CRT. © 2004 Elsevier Inc.**

**Hepatocellular carcinoma, Radiation-induced liver disease, Normal tissue complication probability, Hepatitis B virus carrier.**

## INTRODUCTION

Hepatocellular carcinoma (HCC) is one of the most common malignancies in the world (1). Several modalities, including surgery, percutaneous ethanol intratumor injection therapy, transcatheter arterial chemoembolization (TACE), radiofrequency ablation, radiotherapy (RT), and chemotherapy, have been used in treating HCC patients (2, 3). Three-dimensional conformal RT (3D-CRT) has been integrated into multimodality therapy in specific situations in the past few years (4–6). The improvement in outcome as a result of dose escalation and appropriate selection of

patients who may benefit from 3D-CRT has been somewhat encouraging (7, 8). In addition to the possible change in the patterns of failure, the 3D-CRT–related side effects deserve much attention (8). Radiation-induced liver disease (RILD) is one of the most frequently encountered complications (9). The clinical presentations and dosimetric implications have been reported in different series (10, 11). The computerized treatment design plays an essential role in generating dose–volume data and in estimating the probability of RILD (10). The estimates of the Lyman normal tissue complication probability (NTCP) parameters have correlated well with the risk of RILD in patients who completed 3D-CRT (12,

---

13). Nondosimetric factors, such as the origin of malignant disease and the regimens of concomitant chemotherapy, were also associated with RILD (12). However, the determining factors and their impact on the probability of RILD were not identical in different series, especially for Asian patients with prevalent chronic viral hepatitis and its pathogenesis-related HCC (13). In this study, we retrospectively reviewed the clinical evidence of RILD and the treatment plans of 89 patients who exclusively had HCC and had undergone 3D-CRT. We analyzed the clinical, biologic, and dosimetric factors with a statistically significant impact on the occurrence of RILD. The implication of Lyman's NTCP model with the parameters best fitting the true condition of these patients was also investigated.

## METHODS AND MATERIALS

### Patients and follow-up

Between November 1993 and December 2001, 134 patients completed external beam radiotherapy to part of the liver at our institution. Of the 134 patients, 45 were excluded from this study because of a diagnosis other than HCC (*n* = 30), incomplete dose–volume data for the palliative treatment (*n* = 10), or a follow-up interval of <4 months after completion of 3D-CRT (*n* = 5). The study included the remaining 89 patients. Of the 89 patients, 78 (88%) had a histologic diagnosis of HCC before treatment, and 11 had refused hepatic tumor biopsy or fine needle aspiration. However, patients with no tissue diagnosis had imaging findings compatible with HCC and a high serum α-fetoprotein level of >400 ng/mL. Sixty-five patients (73%) had a serum virology diagnosis of type B chronic hepatitis, defined as positive hepatitis B virus (HBV) surface antigen (>4 ng/mL by microparticle enzyme immunoassay). Nineteen patients (21%) had positive serum anti-hepatitis C virus results. None of the 89 patients had Child-Pugh Class C cirrhosis of the liver before 3D-CRT. Three patients had regional lymph node metastasis and eight also had extrahepatic distant metastasis and underwent hepatic RT to halt progression at the main liver tumor site. In addition to 3D-CRT, 74 patients underwent TACE, including 39 patients before 3D-CRT, 7 after 3D-CRT, and 28 both before and after 3D-CRT. The median number of courses of TACE was 2 (range, 1–11). Eight patients underwent percutaneous ethanol intratumor injection therapy as a part of their treatment. All 89 patients completed the full course of 3D-CRT and had a follow-up interval of at least 4 months after RT to allow adequate observation of possible RILD. Patients were monitored weekly with physical examination and liver function tests during 3D-CRT. CT scans were obtained before RT, 3–6 weeks after RT completion, and then every 3–6 months, if indicated. The patient characteristics are shown in Table 1.

### Radiotherapy

The entry requirements for RT included (*1*) disease confined to the liver but surgically unresectable owing to main

Table 1. Patient characteristics (*n* = 89)

| Characteristic | Value % |
|---|---|
| Categoric variable | |
| Gender | |
| Male | 64 (72) |
| Female | 25 (28) |
| AJCC stage | |
| II | 27 (30) |
| III | 11 (12) |
| IVA | 44 (50) |
| IVB | 7 (8) |
| T stage | |
| T2 | 26 (29) |
| T3 | 13 (15) |
| T4 | 50 (56) |
| N stage | |
| N0 | 86 (97) |
| N1 | 3 (3) |
| M stage | |
| M0 | 81 (91) |
| M1 | 8 (9) |
| Serum alpha-fetoprotein level (ng/mL) | |
| <20 | 23 (26) |
| 20–200 | 20 (22) |
| 200–400 | 5 (6) |
| 400–1000 | 7 (8) |
| 1000–10000 | 14 (16) |
| >10000 | 20 (22) |
| Chronic hepatitis B viral carrier | |
| Yes | 65 (73) |
| No | 24 (27) |
| Child-Pugh classification for liver cirrhosis | |
| A | 68 (76) |
| B | 21 (24) |
| TACE | |
| Before RT | 39 (44) |
| After RT | 7 (8) |
| Before and after RT | 28 (31) |
| None | 15 (17) |
| PEIT | |
| Yes | 8 (9) |
| No | 81 (91) |
| Continuous variable | |
| Age | |
| Mean ± SD | 56.5 ± 13.1 |
| Range | 19.4–82.2 |
| Isocenter dose (Gy) | |
| Mean ± SD | 49.9 ± 6.2 |
| Range | 36.0–66.0 |
| Gross tumor volume (cm³) | |
| Mean ± SD | 683.7 ± 737.9 |
| Range | 7–4529 |
| Normal liver volume (cm³) | |
| Mean ± SD | 1153.4 ± 350.2 |
| Range | 614–2907 |

*Abbreviations:* AJCC = American Joint Committee on Cancer; TACE = transcatheter arterial chemoembolization; RT = radiotherapy; PEIT = percutaneous ethanol injection therapy; SD = standard deviation.

Data presented as number of patients, with percentage in parentheses, unless otherwise noted.

portal vein thrombosis, inferior vena cava invasion, main hepatic vein invasion, obstructive jaundice, or tumor involv-

ing one or both lobes of the liver with inadequate hepatic function reserve for surgery; (2) Karnofsky performance scale $\geq$70%; (3) indocyanine green retention rate $\leq$30% at 15 min; (4) absence of uncontrollable ascites unresponsive to diuretics and albumin supplement; and (5) no prior RT to the liver. No patient was given RT to the whole liver. For patients with TACE as a part of their treatment, an interval of at least 30 days between TACE and 3D-CRT was necessary, irrespective of which treatment was given first to allow adequate recovery of hepatic function. The mixture of iodized oil contrast medium (Lipiodol) and chemotherapeutic agents consisting of doxorubicin, cisplatin, and mitomycin-C was used for infusion simultaneously with embolization during TACE. Ivalon particles or gelatin sponge particles were used as the embolization material. The radiation technique and dose–volume criteria have been previously reported (6). In brief, the gross tumor volume was defined as the hepatic tumor volume, visualized by three-dimensional computation of contrast-enhanced CT-defined contours. The respiratory movement estimated fluoroscopically in simulation was taken into account when planning the target volume. Nonneoplastic normal liver was defined as the total liver volume minus the gross tumor volume. The radiation portals were generally designed to include the gross tumor volume with 1.5–2-cm margins, with specific modifications to cover the planning target volume. The planning target volume margins were usually 1–2 cm around the clinical target volume, depending on the immobilization device, breathing control mode, and individual respiratory amplitude. RT was delivered with a 6-MV or 18-MV linear accelerator. The mean radiation dose to the isocenter was $49.9 \pm 6.2$ Gy (range, 36.0–66.0 Gy) in daily fractions of 1.8–3 Gy. All but 3 patients had a daily fraction of 1.8–2 Gy. The doses of all patients, including the 2 patients who received daily fractions of 3 Gy and the 1 patient who received a daily fraction of 2.5 Gy, were converted to the normalized isobiologic effective dose of 2 Gy/fraction using the linear-quadratic model with an $\alpha/\beta$ ratio of 2 Gy for the dosimetric computation. The spatial design of the coplanar and non–coplanar beam combination was made using the beam's eye view reconstructed from a CT-based simulation. Dose–volume histograms of the targets and organs at risk were generated from the FOCUS treatment planning system (CMS, St. Louis, MO) in each patient.

### RILD definition

Patients were evaluated for evidence of RILD within 4 months after 3D-CRT completion. RILD was defined as Grade 3 or greater hepatic toxicity according to the Common Toxicity Criteria, version 2.0, of the National Cancer Institute (14) in the absence of documented progressive disease. Progressive disease was assessed by imaging studies and paracentesis of ascites if present. Some patients had an elevated serum level of transaminases compatible with their malignant disease activity before 3D-CRT. Because the Common Toxicity Criteria do not specify the definition

for patients with preexisting abnormal hepatic function, we modified the Grade 3 hepatic toxicity definition on the basis of our previous clinical observation of RILD (11). The hepatic toxicity of these patients was determined on the basis of transaminases elevated to at least five times the pretreatment baseline, rather than the upper limits of the normal range. The clinical manifestations, serum biochemistries, and latent period of RILD have been previously described (11).

### Dosimetric analysis

Several parameters, including the percentage of volume of nonneoplastic liver that received a radiation dose >30 Gy ($V_{30}$), mean radiation dose to the liver, and Lyman NTCP, were obtained from the dose–volume histograms. The mean radiation dose to the liver was calculated by dividing the sum of doses to all voxels of nonneoplastic liver by the number of voxels. The Lyman NTCP model (15) was used:

$$NTCP = 1/\sqrt{2\pi} \int_{-\infty}^{t} \exp(-t^2 2)dt$$

$$t = [D - TD_{50}(v)]/[m \times TD_{50}(v)]$$

$$V = V/V_{ref}$$

The data were fit to the Lyman NTCP model, which describes the probability of a complication after uniform radiation of a fractional volume of normal tissue (v) to a dose (D), assuming a sigmoid dose–response relationship with no threshold. $TD_{50}(v)$ represents the tolerances doses associated with a 50% chance of complications for uniform partial liver RT, where $TD_{50}(v)$ is related to the whole liver (v = 1) tolerance through the power law relationship:

$$TD_{50}(1) = TD_{50}(v) \times V^n$$

where $V_{ref}$ is the volume of nonneoplastic liver; "n" is the volume effect parameter, which relates the tolerance doses of uniform whole organ RT to uniform partial organ RT; and "m" is the steepness of the dose–response at $TD_{50}(1)$. When n is near 1, the volume effect is large and when it is near 0, the volume effect is small. For uniform partial organ RT, the effective volume method of Kutcher and Burman (16) was used to provide estimates of equivalent dose and volume pairs from the dose–volume histograms summarizing the nonuniform RT. The partial volume dose–complication risk relationship for the liver was graphically displayed in dose–effective volume plots (as a function of NTCP).

The three parameters, $TD_{50}(1)$, n, and m, were adjusted to best fit the condition (with or without RILD) in each patient, using the maximal likelihood method (17–19). Confidence intervals of the parameters were determined by the profile likelihood method (20).

Laboratory Data



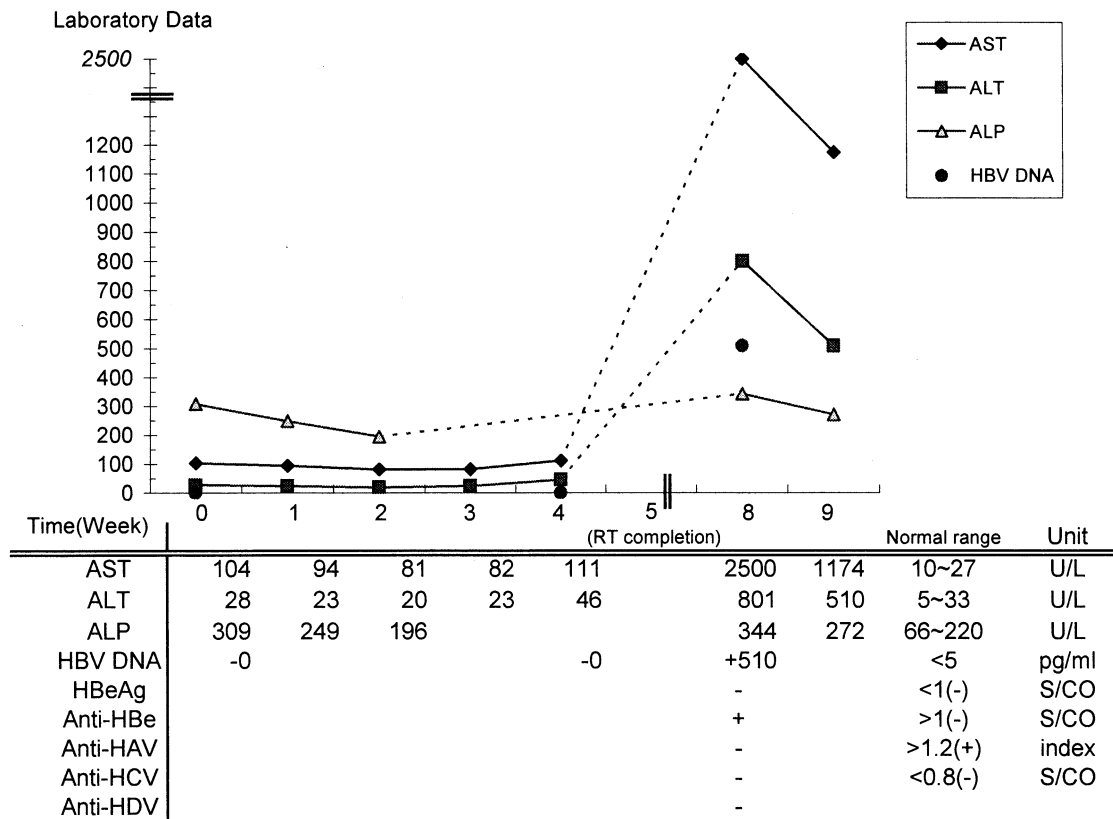| Time(Week) | 0 | 1 | 2 | 3 | 4 | (RT completion) | 8 | 9 | Normal range | Unit |
|---|---|---|---|---|---|---|---|---|---|---|
| AST | 104 | 94 | 81 | 82 | 111 | | 2500 | 1174 | 10~27 | U/L |
| ALT | 28 | 23 | 20 | 23 | 46 | | 801 | 510 | 5~33 | U/L |
| ALP | 309 | 249 | 196 | | | | 344 | 272 | 66~220 | U/L |
| HBV DNA | -0 | | | | -0 | | +510 | | <5 | pg/ml |
| HBeAg | | | | | | | - | | <1(-) | S/CO |
| Anti-HBe | | | | | | | + | | >1(-) | S/CO |
| Anti-HAV | | | | | | | - | | >1.2(+) | index |
| Anti-HCV | | | | | | | - | | <0.8(-) | S/CO |
| Anti-HDV | | | | | | | - | | | |

Fig. 1. Sequential laboratory data of 66-year-old female hepatitis B virus (HBV) carrier, with 12-cm hepatocellular carcinoma at right hepatic lobe, who underwent three-dimensional conformal radiotherapy with 50 Gy. She developed radiation-induced liver disease serologically compatible with reactivation of HBV, 3 weeks after radiotherapy (RT) completion. She was treated with lamivudine but died of hepatic failure 10 days later.

*Clinical and dosimetric factors associated with RILD*

The patient-related, treatment-related, and dosimetry-related factors were analyzed for the correlation with RILD. In univariate analysis, Student's *t* test was used to compare the continuous variables between patients with and without RILD, and the chi-square test or Fisher's exact test was used to compare the categorical variables. Logistic regression analysis was used to investigate the multivariate impact on the occurrence of RILD. $p < 0.05$ resulting from two-sided tests was considered statistically significant. The adjusted parameters of the Lyman NTCP model were again obtained by subgrouping patients on the basis of nondosimetric factors that correlated significantly with RILD. Goodness-of-fit analysis (12) was used to estimate the deviances of the NTCP model parameters of the subgroups from the parameters of the entire group, the group in the University of Michigan series (12), and groups in the original literature (21), and to estimate the statistical significance of these deviances.

**RESULTS**

Of the 89 patients, 17 developed RILD after 3D-CRT, compatible with Grade 3 or greater hepatic toxicity. The manifestations were mainly more than a fivefold increase in either transaminases or alkaline phosphatase. Of the 17 patients, 15 presented predominantly with elevated serum transaminases and 2 predominantly with elevated alkaline phosphatase and simultaneous development of ascites. The malignant disease of the 17 patients was not progressing at the development of RILD. The results of the test for HBV DNA revealed that the 2 patients treated in 2001 also had evidence of acute reactivation of chronic hepatitis B (i.e., elevated serum HBV DNA levels [>5 pg/mL by hybridization antibody capture assay]) during RILD. One of these 2 patients with RILD underwent liver biopsy, which revealed the pathologic features of lymphocytic infiltration in the portal areas, periportal piecemeal necrosis, limiting plate destruction, Kupffer cell hyperplasia, and apoptotic eosinophilic bodies within the lobules. All 17 patients with RILD were treated conservatively, and the 2 patients with documented reactivation of viral hepatitis during RILD were also given antiviral medication (lamivudine 100 mg, once daily). Of the 17 patients with RILD, 7 died of it and 10 recovered. One of the 2 patients with elevated serum HBV DNA was treated with antiviral medication and recovered, but the other died of hepatic failure resulting from RILD. The sequential laboratory data of this patient are shown in Fig. 1.

In univariate analysis, chronic HBV carrier status and the mean radiation dose to the liver were significantly associated with the occurrence of RILD. Of the 65 patients who were chronic HBV carriers, 16 developed RILD compared with 1 of the 24 patients who were not ($p = 0.034$). The mean radiation dose to the liver in patients with RILD was significantly greater than that in patients without RILD (22.9 vs. 19.0 Gy, $p = 0.050$). Gender, age, Child-Pugh classification of liver cirrhosis, serum $\alpha$-fetoprotein level, American Joint Committee on Cancer stage, treatment modality with TACE or percutaneous ethanol intratumor injection therapy, gross tumor volume, nonneoplastic liver volume, prescribed isocenter dose, and $V_{30}$ were not associated with the development of RILD (Table 2). In the multivariate analysis of four variables (HBV carrier, Child-Pugh classification, mean radiation dose to liver, and $V_{30}$) showing statistical significance or borderline statistical significance in the univariate test for the model, the correlation of HBV carrier (odds ratio, 9.26; $p = 0.040$) and Child-Pugh B classification (odds ratio, 3.65; $p = 0.036$) with RILD remained statistically significant (Table 3). In the univariate and multivariate analyses of the four subgroups divided on the basis of HBV carrier status and Child-Pugh classification, none of the associations with patient-related and treatment-related factors reached statistical significance in the association with RILD.

For the whole group of 89 patients, the estimated Lyman NTCP model parameters were $TD_{50}(1) = 49.4$ Gy, m = 0.39, and n = 0.35. For the subgroup of 65 HBV carriers, the estimated parameters were $TD_{50}(1) = 50.0$ Gy, m = 0.40, and n = 0.26. By contrast, the estimated parameters of the 24 who were not HBV carriers were $TD_{50}(1) = 46.1$ Gy, m = 0.31, and n = 0.86 (Fig. 2). For the subgroup of 68 Child-Pugh Class A patients, the estimated parameters were $TD_{50}(1) = 48.9$ Gy, m = 0.30, and n = 0.35, and the estimated parameters of the 21 Child-Pugh Class B patients were $TD_{50}(1) = 38.7$ Gy, m = 0.22, and n = 0.23 (Fig. 3). In addition, the HBV carrier subgroup of 51 patients who were also Child-Pugh Class A, the estimated parameters were $TD_{50}(1) = 47.4$ Gy, m = 0.30, and n = 0.30 (Table 4).

When we compared our 89 patients with those in other series, the goodness of fit (deviance) for our estimated parameter set was 35.7 ($p > 0.995$). The deviance (42.6, $p > 0.995$) was similar to that when using the parameter set ($TD_{50}(1) = 40$ Gy, m = 0.15, n = 0.32) from the original Lyman NTCP model (21). However, the fit (deviance = 106.8, $p < 0.001$) would have been significantly worse with the parameter set ($TD_{50}(1) = 39.8$ Gy, m = 0.12, n = 0.97) from the patients with primary hepatobiliary cancer in the University of Michigan series (12). The comparison for the 65-patient HBV carrier subgroup also showed a similar fit with our parameter set (deviance = 30.1, $p > 0.995$) and the original Lyman model set (deviance = 37.3, $p > 0.995$), but a statistically significantly worse fit with the Michigan set (deviance = 98.9, $p < 0.001$).

Table 2. Univariate analysis for patient-, treatment-, and dosimetry-related variables associated with RILD

| Variable | RILD ($n = 17$) | No RILD ($n = 72$) | p |
|---|---|---|---|
| Gender | | | |
| Male | 14 | 50 | 0.377 |
| Female | 3 | 22 | |
| Age (y) | 58.4 ± 8.5 | 56.0 ± 13.9 | 0.382 |
| Serum alpha-fetoprotein level (ng/mL) | | | |
| <400 | 10 | 38 | 0.653 |
| >400 | 7 | 34 | |
| HBV carrier | | | |
| Yes | 16 | 49 | 0.034 |
| No | 1 | 23 | |
| HCV carrier | | | |
| Yes | 0 | 19 | 0.018 |
| No | 17 | 53 | |
| Child-Pugh classification | | | |
| A | 10 | 58 | 0.108 |
| B | 7 | 14 | |
| AJCC stage | | | |
| II–III | 6 | 32 | 0.493 |
| IVA–IVB | 11 | 40 | |
| T stage | | | |
| T2–T3 | 6 | 33 | 0.431 |
| T4 | 11 | 39 | |
| N stage (N0/N1) | | | |
| N0 | 17 | 69 | 1.0 |
| N1 | 0 | 3 | |
| M stage (M0/M1) | | | |
| M0 | 16 | 65 | 1.0 |
| M1 | 1 | 7 | |
| TACE | | | |
| Yes | 13 | 61 | 0.474 |
| No | 4 | 11 | |
| PEIT | | | |
| Yes | 1 | 7 | 1.0 |
| No | 16 | 65 | |
| Gross tumor volume (cm³) | 623.1 ± 574.0 | 697.9 ± 774.3 | 0.709 |
| Normal liver volume (cm³) | 1144.1 ± 288.4 | 1155.5 ± 365.0 | 0.904 |
| Isocenter dose (Gy) | 49.8 ± 4.1 | 49.9 ± 6.6 | 0.941 |
| $V_{30}$ (%) | 38.6 ± 15.7 | 31.8 ± 14.3 | 0.085 |
| Mean radiation dose to liver (Gy) | 22.9 ± 8.0 | 19.0 ± 7.1 | 0.050 |

*Abbreviations:* RILD = radiation-induced liver disease; HBV = hepatitis B virus; HCV = hepatitis C virus; $V_{30}$ = percentage of volume of normal liver receiving radiation dose >30 Gy; other abbreviations as in Table 1.

## DISCUSSION

With the integration of RT into multimodality treatment for HCC, the issues of dose escalation and risk reduction of treatment-related complications become more important. The University of Michigan and Korean (7, 22, 23) studies of dose-escalation risk emphasized improved outcome with higher doses. The higher radiation dose was associated with more prominent tumor shrinkage, but this effect was probably at the expense of more frequent treatment-related com-

Table 3. Multivariate analysis of variables associated with RILD

| Variable | p | Odds ratio | 95% CI |
|---|---|---|---|
| HBV carrier | 0.040 | 9.3 | 1.1–77.7 |
| Child-Pugh classification B | 0.036 | 3.7 | 1.1–12.2 |
| Mean radiation dose to liver | NS | — | — |
| $V_{30}$ | NS | — | — |

*Abbreviations:* CI = confidence interval; NS = not statistically significant; other abbreviations as in Table 2.

plications. In addition, with combined TACE and 3D-CRT, local control of the large hepatic tumors was similar to that of smaller tumors treated with TACE alone. However, intrahepatic recurrence and, more likely, extrahepatic metastasis deserve further attention (8).

Radiation-induced liver disease, like subacute radiation injury to the liver, has been characterized as a venoocclusive disease (9). It may cause the deterioration of hepatic function and reserve, which is associated with a poor prognosis in HCC patients (24, 25), and high morbidity and mortality, with nearly one-half of RILD patients dying of this complication (11). As the pathophysiology of RILD has become better understood, patient care has improved and mortality in updated series has decreased.

The dosimetric method to describe the probability of RILD has been used in several series. Lawrence *et al.* (10) first modified the volume effect parameter of the liver in the Lyman NTCP model by grouping patients and by narrowing the difference between the estimated NTCP and the observed incidence of RILD. They found that the incidence of

RILD correlated with both the mean radiation dose to the liver and the NTCP. The observed volume effect of the liver (0.79) was much larger than originally estimated (0.32) (21). The updated Michigan series (12) again showed the large volume effect of this organ. More importantly, Lawrence *et al.* (10) showed the significance of nondosimetric factors (including the underlying malignancy of the hepatic tumor and the regimen of concomitant chemotherapy) on RILD. The parameter sets were divided on the basis of the significant factors, with $TD_{50}(1)$ 39.8 Gy and 45.8 Gy for primary hepatobiliary cancer and liver metastasis, respectively. These findings emphasized the importance of grouping patients by patient- or treatment-related variables before doing the dosimetric analysis.

However, the volume effect parameter (0.35) in our patients was much smaller than that in the Michigan series (12), but similar to the original estimates (21). In the early series with whole liver RT, the original small-volume effect (21) may have been due to the poor compensation of subunits of the irradiated liver. Our patients had HCC exclusively, and most were HBV carriers. The subclinical and ongoing cirrhosis of the liver is a unique background condition that may lower tolerance of even part of the liver to RT. In the current series, two biologic factors, HBV carrier status and Child-Pugh Class B status, became statistically significant in the correlation with RILD. In the subgroup analyses, association of the dosimetric factors with RILD was not statistically significant, in part because of the small number of patients in each subgroup and the consequent limited statistical power. The difference in volume effect
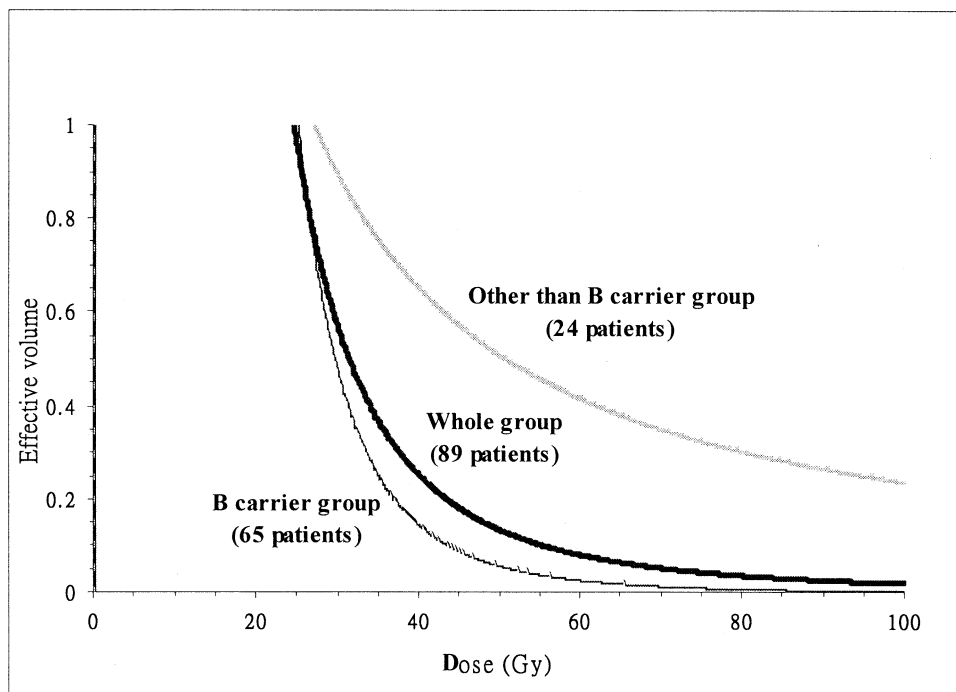


Fig. 2. Iso-normal tissue complication probability (NTCP) (10%) curve comparison of fits from whole group (*n* = 89), subgroup of hepatitis B virus (HBV) carriers (*n* = 65), and subgroup of remaining patients (*n* = 24).
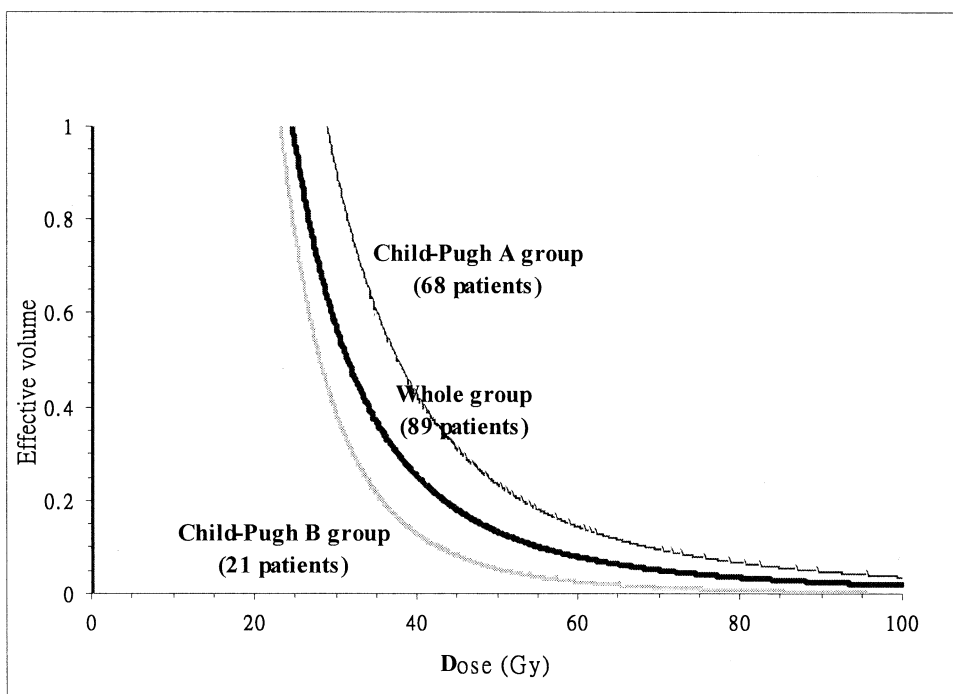
Fig. 3. Iso-normal tissue complication probability (NTCP) (10%) curve comparison of fits from whole group ($n = 89$) and subgroups with Child-Pugh Class A ($n = 68$) and Child-Pugh Class B ($n = 21$) liver cirrhosis.

(0.26 vs. 0.86) was large after dividing patients according to their HBV carrier status. The small-volume effect of the liver was mainly from the HBV carriers. In contrast, the volume effect parameter in patients other than HBV carriers was the same as that in the Michigan series. These findings mean that the susceptibility to, and even pathogenesis of, RILD may be different in HBV carriers and noncarriers.

Our previous report also described the clinical manifestations of 12 HCC patients with RILD after 3D-CRT (11). Of the 11 HBV carriers, 10 presented with elevated transaminases rather than the commonly reported increase in alkaline phosphatase. This finding implies that radiation damage occurred more often in the hepatocytes than in the bile ducts. The striking clinical difference again supports the possibility that RILD induction is via a unique pathway in HBV carriers. The serologic evidence of reactivation of HBV in 2 patients (3D-CRT plus RILD) indicated the possibility that reactivation of viral hepatitis was the underlying cause of RILD, although we have no data for the other

15 patients treated before 2001. Because we were able to test and obtain serologic evidence of HBV reactivation in only 2 of our RILD patients, it was impossible to assess the hypothesis that HBV plays a role in RILD pathogenesis. Whether RT to part of the liver, like chemotherapy, reactivates HBV deserves further investigation. Sequential serologic tests during and after 3D-CRT and clinical observation of RILD are urgently needed in future protocols, especially for Asian patients with prevalent chronic viral hepatitis B.

The Child-Pugh classification, widely used in evaluating hepatic functional reserve (26), was also significantly associated with RILD. Hepatic function is not only a selection criterion, but also a prognostic factor for HCC patients (24, 25). RT, like the other modalities, may partially compromise the hepatic reserve (27). Both HBV carrier status and Child-Pugh classification were independent factors in multivariate analyses and, therefore, have individual influence on the risk of developing RILD. It is likely that HBV carriers developed RILD through a specific process trig-

Table 4. Lyman NTCP model parameters of whole group and subgroups

| Parameters | Whole group ($n = 89$) | HBV carrier ($n = 65$) | Not HBV carrier ($n = 24$) | Child A cirrhosis ($n = 68$) | Child B cirrhosis ($n = 21$) | HBV and Child A ($n = 51$) |
|---|---|---|---|---|---|---|
| $TD_{50}(1)$ (Gy) | 49.4 (42.0–60.5) | 50.0 (42.0–62.0) | 46.1 (15.0–>70) | 48.9 (42.0–59.0) | 38.7 (33.9–45.1) | 47.4 (42.0–57.2) |
| m | 0.39 (0.28–0.58) | 0.40 (0.27–0.73) | 0.31 (0.18–0.60) | 0.30 (0.22–0.45) | 0.22 (0.10–1.52) | 0.30 (0.20–0.52) |
| n | 0.35 (0.20–0.58) | 0.26 (0.13–0.48) | 0.86 (0.33–>2) | 0.35 (0.21–0.58) | 0.23 (0.14–0.36) | 0.30 (0.17–0.50) |

*Abbreviations:* NTCP = normal tissue complication probability; $TD_{50}(1)$ = 50% tolerance dose for uniform irradiation of whole liver; m = steepness of dose–complication curve for fixed partial volume; n = volume effect parameter; HBV = hepatitis B virus.

Data in parentheses are 95% confidence intervals.

gered by RT to part of the liver, but this process was not limited to functional compromise of the liver.

Most of our patients in this study underwent TACE as a part of their treatment, with the interval requirement of at least 1 month between TACE and 3D-CRT. This protocol design was based on the commonly used interval between repeated courses of TACE for patients with HCC or liver metastasis, with acceptable recovery of hepatic function (28). With the regional pattern of TACE and its insignificance in association with RILD in our statistical analysis, it is not likely that it has a significant effect on the occurrence of RILD.

The patient population, clinical manifestation of liver toxicity, and treatment modality were different between this study and the previously reported series. The unique dosimetric and biologic findings are important but are probably specific to Asian patients. The dosimetric factors, such as the mean liver dose and Lyman NTCP, were still useful in our patients (13). The dosimetric indicators were more effective after grouping patients by the biologic factors. Some interpretations of this study were still limited because of the relatively small number of patients, especially non-HBV carriers. The small number in each subgroup widened the confidence interval and resulted in somewhat inconsistent estimates in the likelihood analysis. However, recruiting many non-HBV carrier patients with HCC undergoing 3D-CRT in Asia may not be easy, especially with the strict selection criteria used in our protocol. Additional follow-up with more patients in these subgroups is needed to confirm estimates.

## REFERENCES

1. Cook GC, Moosa B. Hepatocellular carcinoma: One of the world's most common malignancies. *Am J Med* 1985;233:705–708.
2. Tsuzuki T, Sugioka A, Ueda M. Hepatic resection for hepatocellular carcinoma. *Surgery* 1990;107:511–520.
3. Ohto M, Yoshikawa M, Saisho H, *et al.* Non surgical treatment of hepatocellular carcinoma in cirrhotic patients. *World J Surg* 1995;19:42–1946.
4. Robertson JM, Lawrence TS, Andrews JC, *et al.* Long-term results of hepatic artery fluorodeoxyuridine and conformal radiation therapy for primary hepatobiliary cancers. *Int J Radiat Oncol Biol Phys* 1995;37:325–330.
5. Yasuda S, Ito H, Yoshikawa M, *et al.* Radiotherapy for large hepatocellular carcinoma combined with transcatheter arterial embolization and percutaneous ethanol injection therapy. *Int J Oncol* 1999;15:467–473.
6. Cheng JC, Chuang VP, Cheng SH, *et al.* Local radiotherapy with or without transcatheter arterial chemoembolization for patients with unresectable hepatocellular carcinoma. *Int J Radiat Oncol Biol Phys* 2000;47:435–442.
7. Dawson LA, McGinn CJ, Normolle D, *et al.* Escalated focal liver radiation and concurrent hepatic artery fluorodeoxyuridine for unresectable intrahepatic malignancies. *J Clin Oncol* 2000;18:2210–2218.
8. Cheng JC, Chuang VP, Cheng SH, *et al.* Unresectable hepatocellular carcinoma treated with radiotherapy and/or chemoembolization. *Int J Cancer (Radiat Oncol Invest)* 2001;96:243–252.
9. Lawrence TS, Robertson JM, Anscher MS, *et al.* Hepatic toxicity resulting from cancer treatment. *Int J Radiat Oncol Biol Phys* 1995;31:1237–1248.
10. Lawrence TS, Ten Haken RK, Kessler ML, *et al.* The use of 3-D dose volume analysis to predict radiation hepatitis. *Int J Radiat Oncol Biol Phys* 1992;23:781–788.
11. Cheng JC, Wu J-K, Huang C-M, *et al.* Radiation-induced liver disease after radiotherapy for hepatocellular carcinoma: Clinical manifestation and dosimetric description. *Radiother Oncol* 2002;63:41–45.
12. Dawson LA, Normolle D, Balter JM, *et al.* Analysis of radiation-induced liver disease using the Lyman NTCP model. *Int J Radiat Oncol Biol Phys* 2002;53:810–821.
13. Cheng JC, Wu J-K, Huang C-M, *et al.* Radiation-induced liver disease after three-dimensional conformal radiotherapy for patients with hepatocellular carcinoma: Dosimetric analysis and implication. *Int J Radiat Oncol Biol Phys* 2002;54:156–162.
14. Trotti A, Byhardt R, Stetz J, *et al.* Common Toxicity Criteria, version 2.0. An improved reference for grading the acute effects of cancer treatment: Impact on radiotherapy. *Int J Radiat Oncol Biol Phys* 2000;47:13–47.
15. Lyman JT. Complication probability as assessed from dose volume histograms. *Radiat Res* 1985;8(Suppl.):513–519.
16. Kutcher GJ, Burman C. Calculation of complication probability factors for non-uniform normal tissue irradiation: The effective volume method. *Int J Radiat Oncol Biol Phys* 1989;16:1623–1630.
17. Cox D, Snell E. Analysis of binary data. New York: Chapman and Hall, 1989: p. 179–184.
18. Ross CJS. Nonlinear estimation. New York: Springer-Verlag, 1990.
19. Wetherill GB. Intermediate statistical methods. London: Chapman & Hall, 1981.
20. Roberts SA, Hendry JH. The delay before onset of accelerated tumour cell repopulation during radiotherapy: A direct maximum-likelihood analysis of a collection of worldwide tumour-control data. *Radiother Oncol* 1993;29:69–74.
21. Burman C, Kutcher GJ, Emami B, *et al.* Fitting of normal tissue tolerance data to an analytic function. *Int J Radiat Oncol Biol Phys* 1991;21:123–135.
22. McGinn CJ, Ten Haken RK, Ensminger WD, *et al.* Treatment of intrahepatic cancers with radiation doses based on a normal tissue complication probability model. *J Clin Oncol* 1998;16:2246–2252.
23. Park H, Seong J, Han K, *et al.* Dose–response relationship in local radiotherapy for hepatocellular carcinoma. *Int J Radiat Oncol Biol Phys* 2002;54:150–155.
24. Lau H, Fan ST, Ng IO, *et al.* Long term prognosis after hepatectomy for hepatocellular carcinoma: A survival analysis of 204 consecutive patients. *Cancer* 1998;83:2302–2311.
25. Poon RT, Fan ST, Lo CM, *et al.* Intrahepatic recurrence after curative resection of hepatocellular carcinoma: Long-term results of treatment and prognostic factors. *Ann Surg* 1999;229:216–222.
26. Kim WR, Poterucha JJ, Wiesner RH, *et al.* The relative role of the Child-Pugh classification and the Mayo natural history model in the assessment of survival in patients with primary sclerosing cholangitis. *Hepatology* 1999;29:1643–1648.
27. Matsuura M, Nakajima N, Arai K, *et al.* The usefulness of radiation therapy for hepatocellular carcinoma. *Hepatogastroenterology* 1998;45:791–796.
28. Kawai S, Tani M, Okamura J, *et al.* Prospective and randomized trial of lipiodol-transcatheter arterial chemoembolization for treatment of hepatocellular carcinoma: A comparison of epirubicin and doxorubicin (second cooperative study). *Semin Oncol* 1997;24(2 Suppl. 6):S38–S45.